Structural Eng./Earthquake Eng., JSCE, Vol. 17, No. 1, 37s－46s, 2000 April
(J. Struct. Mech. Earthquake Eng., JSCE, No. 647/ I－51)

PROPOSAL OF HEALTH MONITORING SYSTEM USING ACROSS TECHNOLOGY

Muneo HORI[1] and Yoriyuki YAMASHITA[2]

[1]Earthquake Research Institute, University of Tokyo (Yayoi, Bunkyo, Tokyo 113-0032, Japan)
[2]Nippon Tlegraph and Telephone Company (Uchisaiwai-cho, Chiyoda, Tokyo 100-0011, Japan)

This paper proposes a health monitoring system for structure members using the ACROSS technology that attains a high S/N ratio by accurately controlling small but harmonic signals and stacking data in a longer period. The identification of possible defects are obtained through the inversion based on the equivalent inclusion method. A prototype of the health monitoring system is developed. It is shown in model experiments and numerical simulations that the location of defects can be detected if sufficiently longer stacking is made to analyze waves scattered by the defects. The results support the potential usefulness of the proposed system.

Key Words : *health monitoring, inverse problem, inversion, ACROSS, QNDE*

1. INTRODUCTION

Civil structures suffer deterioration and damage in long service periods due to various causes. The health monitoring is essential, and a quantitative nondestructive evaluation is needed in identifying the occurrence of defects and damages as well as estimating their degree. Such monitoring, however, is not easily made since it requires a large apparatus and may stop services of the structures temporally.

The committee of the applied solid mechanics[1)] in the JSCE summarized a state-of-art on the nondestructive evaluation and the health monitoring. Several problems were pointed out. They were mainly related to the difficulty in measurement; in particular, questions are posed on the reliability, i.e., whether defects can be found or not, or whether the evaluation is correct or not. The committee suggested that new rational methods of health monitoring were required such that a target structure could be routinely examined with low costs.

In geophysics, continuous monitoring is needed for the investigation of faults conditions. A new technology, called ACROSS[2)], *A*ccurately *C*ontrolled *R*outine *O*perated *S*eismic Source *S*ystem, has been proposed to this end; see the study[3)] about ACROSS made in civil engineering. The basic principles of the ACROSS technology are summarized as follows:

1. A source transmits small but accurate harmonic waves continuously as a signal.
2. A receiver stacks data in a long period synchronizing the period with the input signal.

A high S/N ratio can be attained by accurately controlling signals and stacking; see Appendix A. These principles are completely different from conventional methods which must use larger signals for a higher S/N ratio. The application of the ACROSS technology is a candidate for the health monitoring of huge civil structures.

A health monitoring system using the ACROSS technology is proposed in this paper. The system consists of a network of transmitting and receiving signals, and an analysis of measured data to predict possible defects and damages. A prototype is developed by carrying out model experiments and numerical simulations. A measuring apparatus is made for the experiments; harmonic waves are generated by a small stepping motor and synchronized stacking is made by a personal computer. The analysis is the inversion from scattered waves to source defects. A simple numerical method is developed, which first detects the location of the defects if exist, and then evaluates the degree of the defects.

The content of this paper is as follows: The formulation of the ACROSS health monitoring system are briefly summarized in Section 2. The results of the model experiments and the numerical simulations of the monitoring system are presented in Sections 3 and 4, respectively. Concluding remarks are made in Section 5. Note that we use index notation and employ the summation convention to simplify mathematical expressions; an index following a comma stands for the derivative with respect to the corresponding coordinate.

2. FORMULATION

The ACROSS health monitoring system puts purely harmonic signals and measures waves scattered by defects. The measured waves are analyzed to identify the location and degree of the defects. If defects are modeled as the local change of material properties, the system is aimed at finding local heterogeneity from scattered waves in the frequency domain. This problem is usually formulated as a non-linear inverse and may not be solved easily; see references[4),5),6)] for the inverse problems and their analysis; see also references[7)~12)] for the inverse problems considered in the civil engineering. The authors are proposing a new formulation[15)~17)] based on the equivalent inclusion method[13),14)], which results in a pair of linear inverse problems. The formulation is suitable for the ACROSS, as it first determines an apparent harmonic force which causes such scattered waves, and then determines the properties of the scattered waves.

The inverse problem for the ACROSS health monitoring system is set as follows: Consider a simple case when elasticity tensor or density, C_{ijkl} or ρ, varies locally in a plate member. The x_1- and x_2-axes are taken in the plate, and the x_3-axis is normal to the plate. A point on the surface or inside the plate is denoted by $\boldsymbol{x}' = (x_1, x_2)$ or $\boldsymbol{x} = (x_1, x_2, x_3)$, respectively. The following conditions are set when harmonic waves are transmitted and received:

1. A harmonic signal of angular frequency ω is input at one point on the surface.
2. The amplitude of the resulting harmonic displacement is measured at various points on the surface.

For the sake of generality, we model a plate as a three-dimensional elastic body. Denoting by ΔC_{ijkl} or $\Delta\rho$ the change in the elasticity tensor or the density, respectively, we write the governing equation for displacement, u_i, as

$$((C_{ijkl} + \Delta C_{ijkl})u_{k,l})_{,i} + (\rho + \Delta\rho)\omega^2 u_j = 0. \quad (1)$$

Note that external forces which produces waves can be included in Eq. (1) as body forces. According to the equivalent inclusion method, we define *eigenstress* or *eigeninertia* as

$$\sigma^*_{ij} = \Delta C_{ijkl} u_{k,l} \quad (2)$$

$$\mu^*_i = \omega^2 \Delta\rho u_i, \quad (3)$$

such that the effects of heterogeneity are replaced by the equivalent stress or inertia. Then, we rewrite Eq. (1) as

$$\begin{cases} C_{ijkl}u_{k,li} + \rho\omega^2 u_j + b^*_j = 0, \\ b^*_j = \sigma^*_{ij,i} + \mu^*_j. \end{cases} \quad (4)$$

Here, b^*_i is an apparent body force, and called an *eigen-body-force* which represents the effects of the heterogeneities.

Boundary conditions are required in order to compute u_i by solving Eq. (4) for given b^*_i. However, b^*_i can be determined without considering boundary conditions when u_i is measured densely; indeed, the first two terms of Eq. (4) give b^*_i as

$$b^*_j = -C_{ijkl}u_{k,li} - \rho\omega^2 u_j. \quad (5)$$

By definition, Eqs. (2) and (3), the eigen-body-force b^*_i is generated only where defects exit. The properties of the defects can be determined by examining b^*_i's which are obtained for various frequencies.

Now, we treat the body as an isotropic plate, and consider a case when the change in Young's moduli or density, ΔE or $\Delta\rho$, is uniform in the x_3-direction, i.e., $\Delta E(\boldsymbol{x}')$ or $\Delta\rho(\boldsymbol{x}')$. We assume that in-plane displacement components, u_1 and u_2, are smaller than the out-of-plane displacement component, and that the out-of-plane displacement is uniform in the x_3-direction. Then, we can reduce Eq. (4) and obtain a governing equationfor u_3, making use of Eqs. (2) and (3), as follows:

$$\begin{cases} C_{i33l}u_{3,il} + \rho\omega^2 u_3 + b^*_3 \approx 0, \\ b^*_3 \approx (\Delta C_{i33l}u_{3,l})_{,i} + \Delta\rho\omega^2 u_3, \end{cases} \quad (6)$$

where ΔC_{ijkl}, $\Delta\rho$ and u_3 are functions of $\boldsymbol{x}'$, and a suffix i or l takes on either 1 or 2. Note that the plate theory yields a bi-harmonic governing equation for u_3, using these two assumptions; in this paper, Eq. (6) is used only for the simplicity and similar inversion can be made when the bi-harmonic governing equation is used. Furthermore, denoting the measured displacement by $\overline{u}_3$, we simplify Eq. (5) as

$$b^*_3 \approx -C_{i33l}\overline{u}_{3,il} + \rho\omega^2\overline{u}_3. \quad (7)$$

Provided that either only ΔC_{ijkl} or $\Delta\rho$ (not both) is present, we can determine

$$(\Delta C_{i33l}\overline{u}_{3,l})_{,i} = b^*_3, \quad (8)$$

$$\Delta\rho\omega^2\overline{u}_3 = b^*_3. \quad (9)$$

3. MODEL EXPERIMENTS

The major objective of the model experiments is to study the accuracy of the ACROSS measurement by examining the ability of a source and a receiver. Prototypes of the source and receiver are developed, and they are used to identify a weight, which is used as a model of defect; see **Fig.** 1. The location and the weight are the target of the inversion.

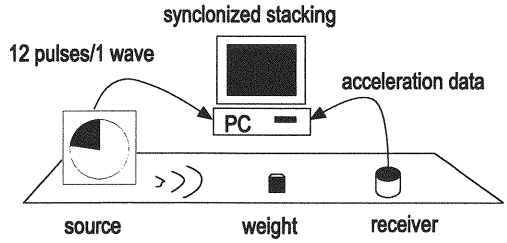

Fig. 1 Model Experiment

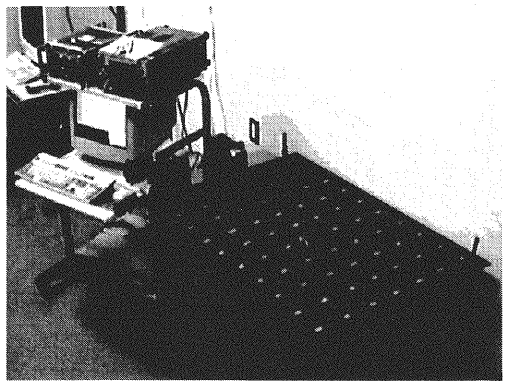

Fig. 2 Experiment Apparatus

(1) Experiment Apparatus

A steel plate of 105×75×0.4cm is used, with the four corners fixed on a table; see **Fig.** 2. As the P-wave velocity of the steel is 6000m/s, the phase change during the wave propagation is negligibly small. A source is a stepping motor which rotates an eccentric weight of $4.14\text{kg}\times10^{-5}\text{kgm}$. The frequency range is 0~50Hz with a relative error 2%; this phase error is adjusted by using 12 pulse signals emitted from the motor during one rotation. A receiver is a piezo-type transducer, and measures a vertical component of the acceleration on the plate surface. The transducer is connected to a PC through an AD board, and stacking is made in accordance with the motor pulse signals. The AD board digitizes ±5V into 65536 segments and the resolution of the acceleration is $3.68\times10^{-4}\text{m/s}^2$. **Table** 1 summarizes the properties of the source and the receivers to control the phase and amplitude of signals.

As a preliminary experiment, we investigate the noise reduction due to stacking. **Figure** 3 plots the standard deviation of measured acceleration in the absence of signals with respect to stacking number N. As expected, the noise decreases as N increases; the dashed line is obtained by assuming that the standard deviation of noises is proportional to $1/\sqrt{N}$ and it is

Table 1 Properties of Source and Receiver

	phase	amplitude
source	2% relative error	4% relative error
receiver	adjusted	$3.68\times10^{-4}\text{m/s}^2$ resolution

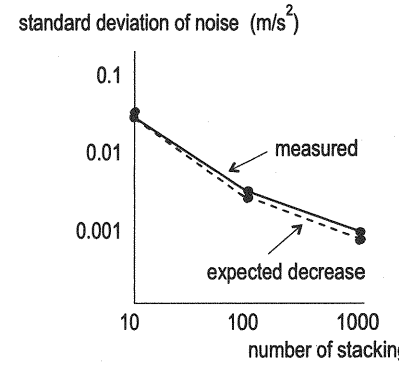

Fig. 3 Noise Reduction due to Stacking

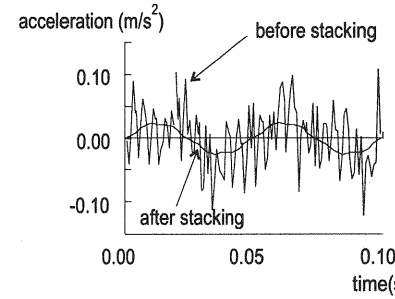

Fig. 4 Waves before and after Stacking

in good agreement with the measured data. Next, we examine the ability of receiving signals. **Figure** 4 shows a typical example of stacked acceleration measured at a receiver in 40cm distance from a source. The frequency is 20Hz, and stacking of 6400 times is made. The harmonic signal appears after this stacking. **Figure** 5 shows the power spectra before and after stacking. It is clearly seen that the long stacking catches a 20Hz component which is hidden in noises before stacking.

(2) Identification of Weight

A weight, which is used as a model of a defect with different density or stiffness, is 0.96kg, and its dimension is 5.0×6.0×5.5cm. The weight is tightly fixed on the plate by a magnet attachment, and can be moved on the plate such that various setting of the defect is studied. The interface of 30cm^2 area can change the

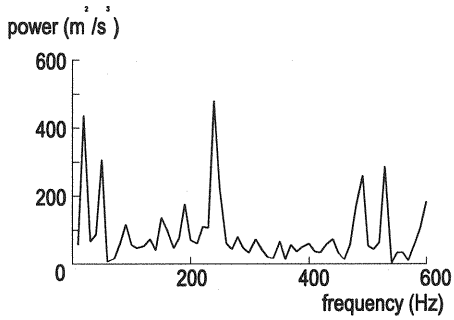

a) before stacking

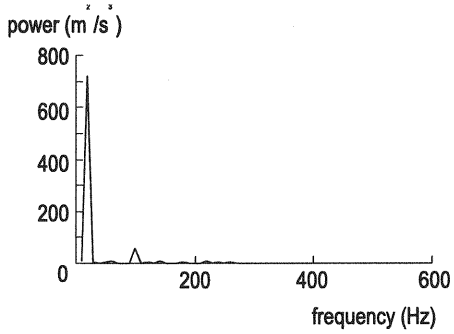

b) after stacking

Fig. 5 Power Spectra of Measured Waves

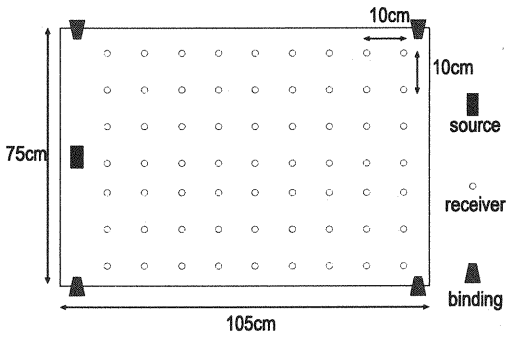

Fig. 6 Location of Measuring Points

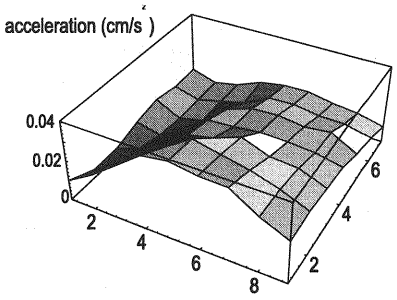

a) absence of weight

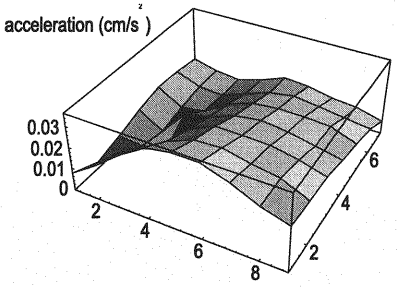

b) presence of weight

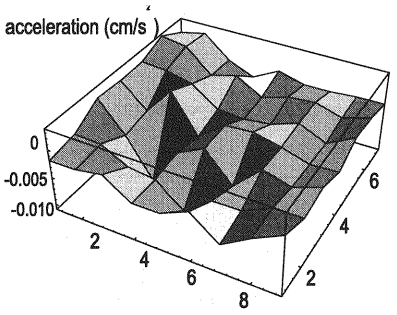

c) difference in acceleration

Fig. 7 Distribution of Measured Acceleration

local density as well as the local stiffness. The vertical acceleration is measured at an array of 63 (=7×9) points in 10cm distance; see **Fig.** 6 for the location of measuring points and the source.

As a typical example of the measurement, **Fig.** 7 shows the distribution of the measured acceleration when signals of 20Hz are input; a) and b) are in the absence and presence of the weight, respectively, and c) is the difference of these distributions. Stacking number is 64, and the relative error of measuring the acceleration is 5%. The motor is put at the coordinate (6,3). Larger change in the acceleration takes place at the measuring points around the weight, even though some changes are observed at other points. Similar change in the acceleration distribution is measured for signals of 15Hz as well. Measuring the change in the acceleration means that some effects of the weight can be obtained through the present prototype of the ACROSS health monitoring system.

For nine measuring points near the weight, we make stacking of 6400 times, such that the accuracy of measuring the acceleration increases up to the resolution of $1.04\times10^{-4}\mathrm{m/s^2}$. The nine points are equally spaced in a square of 20×20cm and the defect is located just right of the center point. **Figure** 8a) shows the resultant of eigen-body-forces computed at points near

the defect (the coordinate is (6,2)) for the input of 15 and 20Hz; see the next section for the detailed explanation of computing the resultant of the eigen-body-forces. The resultant eigen-body-forces at the point far from the defect ((1,1)) are cited for the comparison. **Figure** 8b) shows the difference caused by the presence of the weight. Due to the error in measuring the acceleration, resultant eigen-body-forces of order 10N are computed at points far from the defect. Hence, setting, say, 10N as a critical value, we can judge the presence of the weight using signals of several frequencies if the resultant eigen-body-forces exceed this critical value. The mass of the weight cannotbe determined, as the computed mass is almost zero. The change in the acceleration is probably due to the change in the local stiffness that is caused by the interface between the weight and the plate, not due to the mass of the weight. It is shown from these results that the ACROSS health monitoring system can tell the initiation of defects by examining the change in the measured acceleration. The system can tell the location as well, if suitably large stacking is made for data measured by a dense array of receivers.

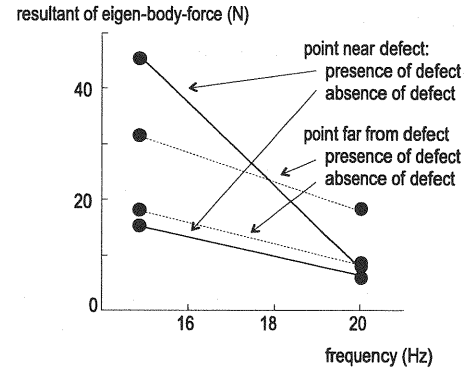

a) resultant eigen-body-force

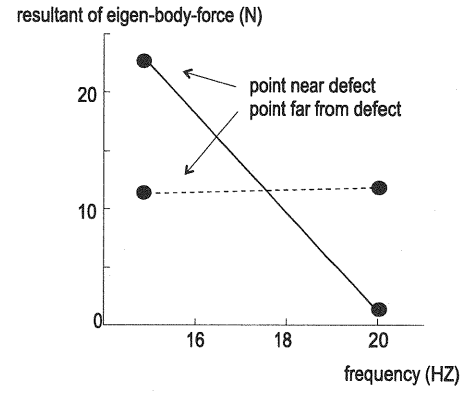

b) difference

Fig. 8 Results of Longer Stacking

4. NUMERICAL SIMULATION

Based on the model experiments, we carry out numerical simulations of identifying defects in a plate using the ACROSS health monitoring system. A pair of linear inverse problems shown in Section 2 are solved by applying an FEM-based numerical computation.

(1) Inversion Using FEM Analysis

According to the ordinary discretization used in the FEM, we write the first inverse problem, Eq. (4), in the following matrix form:

$$[K][U] + \omega^2[M][U] + [F^*] = 0, \tag{10}$$

where $[K]$ and $[M]$ arethe global stiffness and mass matrices, $[U]$ is the global nodal displacement vector, and $[F^*]$ is the global nodal eigen-force vector. We use 8 node isoparametric elements to compute $[K]$, and a diagonal concentrated mass for $[M]$. The nodal eigen-forces are equivalent to the resultant of eigen-body-forces distributed in elements. We write the second inverse problem, Eq. (4), in a similar simple matrix form, as

$$[F^*] = [\Delta K][U] + \omega^2[\Delta M][U] \tag{11}$$

where $[\Delta K]$ and $[\Delta M]$ represent the heterogeneity in the global stiffness and the mass matrices.

While the inverse of the matrices need to be taken to compute $[U]$ in Eq. (10) for a given $[F^*]$, we can directly obtain $[F^*]$ when $[U]$ is given as measured data. Furthermore, we can compute a nodal eigen-force *locally* using displacements which are measured at near-by nodes, such that the equilibrium is satisfied at the corresponding node. Indeed, choosing all elements that share one node, we can compute the nodal eigen-forces as

$$[f^*] = -[k][u] - \omega^2[m][u], \tag{12}$$

where $[f^*]$ is a nodal eigen-force at the node, $[u]$ represents nodal displacements for the elements sharing the node, and $[k]$ and $[m]$ can be determined from the element stiffness and mass matrices. For an eight-node element, $[f^*]$ and $[u]$ are vectors of 3 and $57(= 3 \times 18)$ components and $[k]$ and $[m]$ are 3×54 matrices.

For a thin plate, we can assume that in-plane displacements are zero, and the equilibrium needs to be considered in the x_3-direction only. That is, the x_3 components of nodal eigen-forces are identified from the x_3 components of displacements,

$$f^* = -[k][\overline{u}] - \omega^2[m][\overline{u}], \tag{13}$$

where $[\overline{u}]$ is a vector for measured nine nodal displacement and f^* is a scalar nodal eigen-force.

The inversion from the nodal eigen-force to the heterogeneity is also made through linear matrix algebra. For instance, consider a case when only one element is damaged among four elements that share one node. We assume that the Young modulus and density of the damaged element are $E + \Delta E$ and $\rho + \Delta\rho$, and that the Poisson ratio does not change. In the same manner as Eq. (10) is reduced to Eq. (12), we can reduce Eq. (11) to a *local* form; denoting the element stiffness and mass matrices of the damaged elements by $(E + \Delta E)[\tilde{k}]$ and $(\rho + \Delta\rho)[\tilde{m}]$, with $[\tilde{k}]$ and $[\tilde{m}]$ being the stiffness and mass matrices of $E = 1$ and $\rho = 1$, respectively, we have

$$\Delta E[\tilde{k}][\overline{u}] + \omega^2 \Delta\rho[\tilde{m}][\overline{u}] = f^*, \tag{14}$$

for each frequency. Hence, when f^* is given from Eq. (13), ΔE and $\Delta\rho$ are determined from Eq. (14). It should be noted that while the inversion originally uses differential equations, Eqs. (4) and (5), they can be reduced to Eqs. (13) and (14), which are simple matrix equations. This is one advantage of the pair of the linear inverse problems as these inverse problems are easily discretized in a form used in the FEM.

Matrices $[k]$ and $[m]$ in Eq. (12) may change, depending on the arrangement of a damaged element(s) in elements sharing one node. Also, $[\tilde{k}]$ in Eq. (14) will be changed when, say, the Poisson ratio is changed as well. The form of these matrix equations, however, remains the same even though more computation is required to solve them.

(2) Results of Numerical Simulation

The results of the FEM-based inversion are presented for a steel plate of 100×75×0.4cm. The plate is discretized into 600 (= 20 × 15 × 2) elements of equal dimensions. Young's modulus, Poisson's ratio and density are $E = 2.01 \times 10^{10}\mathrm{N/m^2}$, $\nu = 0.3$ and $\rho = 7.86 \times 10^3\mathrm{kg/m^3}$, respectively. Receivers are put on 336 (=21×16) nodes on the top of the plate.

First, we consider a case when the plate has one defect which changes the stiffness of a certain small part; see **Fig.** 9. In the finite element method, the defect is modeled as one element with reduced Young modulus. The simulation studies 48 cases, four points (I~IV) of the source location, four frequencies (ω =10, 20, 30, 50Hz) of the input signals, and three reduced Young modulus ($\Delta E/E$ =50, 10, 5%). A typical example of measuring eigen-forces is shown in **Fig.** 10; the signal of ω = 20Hz is transmitted from the source at I, and the reduced Young modulus of the defect is $\Delta E/E$ =50%. Based on the model experiments, we set the relative error of measuring the acceleration

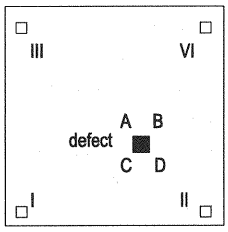

Fig. 9 Location of Defect and Source

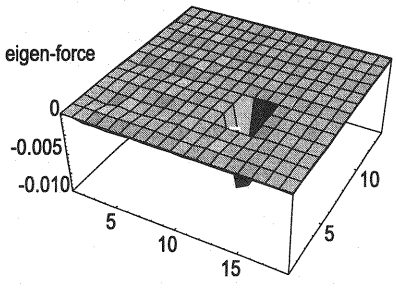

Fig. 10 Distribution of Eigen-Force

as 2%, and neglect eigen-forces smaller than 0.001N as they cannot be distinguished from the error of the measurement. All the four nodes of the element modeling the defect have non-zero eigen-forces. **Table** 2 shows the predicted eigen-force and the associated reduction of Young modulus at the four nodes, A from D, shown in **Fig.** 9. The inversion is satisfactory except for one node; this is because the matrix equation for this node (Eq. (14)) is almost singular and the accuracy of the inversion becomes low. **Table** 3 summarizes the results of the inversion for $\Delta E/E$ =50 and 5%, when signals of ω =10~30Hz are transmitted from the four locations I~IV. It is seen that $\Delta E/E$ can be predicted within 5% error.

Next, we consider a case when there are two defects interacting each other; see **Fig.** 11. All four nodes of the two elements modeling the defects have non-zero eigen-forces. **Table** 4 presents the result of the predicted Young modulus for the defect of $\Delta E/E$ =10%, when the source is put at I~IV and the input frequency is ω =10~30Hz. The error of identifying $\Delta E/E$ is around 2%, which is in agreement with the relative error of 2% accepted in measuring the acceleration. It should be noted that in **Tables** 2 and 3 the predicted value of ΔE does not depend on ω, since the wave length of these frequency is still too long compared with the size of the defect.

Finally, we consider a case when the plate has a crack-like defect. An element modeling the crack is shown in **Fig.** 12; the element is divided into 5 sub-elements and a dark sub-element of 2.5×1×0.2cm rep-

Table 2 Results of Inversion: One Defect (1)

node	f_3^*	$\Delta E/E$
A	.00011	-1.8
B	-.016	-0.5
C	.018	-0.5
D	-.0012	-0.5

Table 3 Results of Inversion: One Defect (2)

a) $\Delta E/E = 5\%$

	I	II	III	IV
10Hz	-7.1	-6.6	-6.8	-8.9
15Hz	-7.1	-6.6	-6.8	-8.9
20Hz	-7.1	-6.6	-6.8	-8.9
30Hz	-7.1	-6.6	-6.8	-8.9

b) $\Delta E/E = 50\%$

	I	II	III	IV
10Hz	-51.9	-50.2	-51.3	-53.5
15Hz	-51.9	-50.2	-51.3	-53.5
20Hz	-51.9	-50.2	-51.3	-53.5
30Hz	-51.9	-50.2	-51.3	-53.5

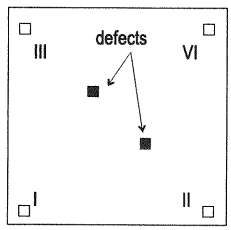

Fig. 11 Case of Two Defects

resents the damage as its Young modulus is decreased. **Figure** 13 shows the eigen-force distribution when the source at I and II (a) and b), respectively) and the frequency of ω =20Hz are used to detect the damage of $\Delta E/E$ =50%. As is seen, the element which has the defect is identified when the same network of 336 receivers is used. The inversion of $\Delta E/E$, however, fails. **Table** 5 summarizes the results of the inversion, presenting $\Delta E/E$ which are determined by using four source locations (I~IV) and four frequencies (10~30Hz). This failure is well understood, since $[\tilde{k}]$ in Eq. (14) is for a uniformly damaged element. It should be noted that while the volume average of $\Delta E/E$ taken over the element is about 10%, the predicted values are much bigger and vary depending on the location of source; this is because the crack-like defect emits strong scattering waves to particular directions.

Table 4 Results of Inversion: Two Defects with $\Delta E/E$=10%

a) defect at left top

	I	II	III	IV
10Hz	-10.4	-10.8	-9.9	-10.2
15Hz	-10.4	-10.8	-9.9	-10.2
20Hz	-10.4	-10.8	-9.9	-10.2
30Hz	-10.4	-10.8	-9.9	-10.2

b) defect at right bottom

	I	II	III	IV
10Hz	-10.2	-10.4	-11.7	-9.3
15Hz	-10.2	-10.6	-11.7	-9.3
20Hz	-10.2	-10.6	-11.7	-9.4
30Hz	-10.2	-10.6	-11.7	-9.3

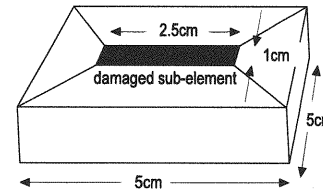

Fig. 12 Model for Crack-Like Defect

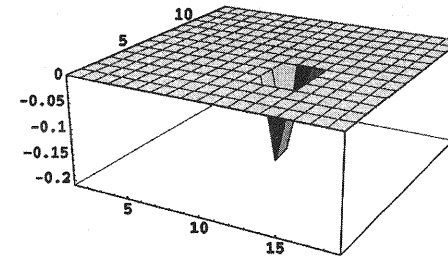

a) source at location I

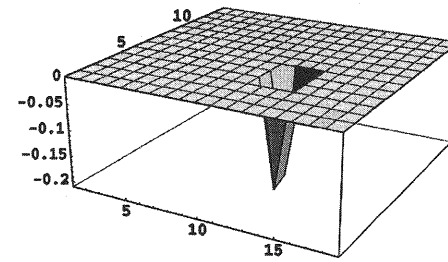

b) source at location II

Fig. 13 Distribution of Eigen-Force

(3) Specifications of Monitoring System

Based on the results of the numerical simulations, we consider specifications of the source and the receiver in a possible actual situation. The major items to be specified are as follows: 1) the frequency of in-

Table 5 Results of Inversion: Crack Defect

	I	II	III	IV
10Hz	-510	-341	-575	-476
15Hz	-510	-341	-575	-476
20Hz	-510	-341	-575	-476
30Hz	-510	-341	-575	-476

put waves; 2) the stacking time; and 3) the spatial arrangement of the sources and receivers.

The numerical simulations show that the accuracy of the inversion does not change much when the frequency of the signal varies between 5 and 30Hz. Hence, it is sufficient to use only one frequency unless much higherfrequencies are applied. The advantage of the ACROSS technology is that the data are in the frequency domain. Hence, it is possible to detect a small change in the acceleration even though signals of relatively low frequencies are input. The stacking time is set such that the amplitude of noises becomes smaller than the minimum resolution of measuring the acceleration. Assuming that noises are at the same level as, say, those measured in the model experiments, we can estimate a required stacking number, N, enough to reduce the acceleration due to noises, as follows:

$$\text{acceleration resolution} = 0.009/\sqrt{N}(\text{m/s}^2). \quad (15)$$

For instance, if the resolution is set as 10^{-4}m/s^2, it requires $N = 6000$ (or 10 minutes stacking) for signals of 10Hz.

While a denser network of sources and receivers is needed for more accurate health monitoring, we can use a coarser network to find at least the initiation of defects. For instance, we consider a network which can identify a defect of 5×5cm and $\Delta E/E$ =10%. In order to evaluate eigen-forces resulting from the measured acceleration distribution, we make numerical simulations similar to the above, setting various arrangement of sources and receivers. **Figure** 14 summarizes these simulations; a) and b), respectively, plot the largest value of computed eigen-forces with respect to the distance of two receivers and the distance between the source and defect. If a critical value of identifying the eigen-force is set by considering the resolution of measuring the acceleration, we can specify the distance of the source and receivers using these plots; for instance, if the critical value is 0.1N (one-tenth of the value used in the model experiments), the smallest distance of receivers and sources are 70cm and 35cm, and hence longer stacking is required to use a coarser network.

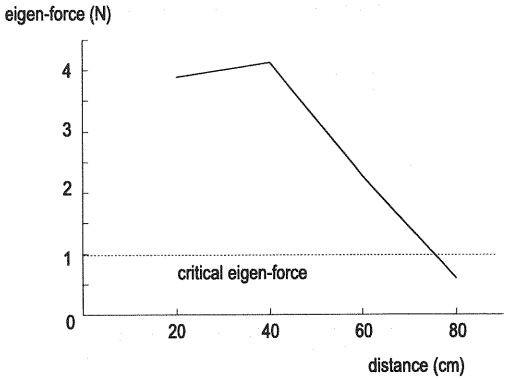

a) change in acceleration

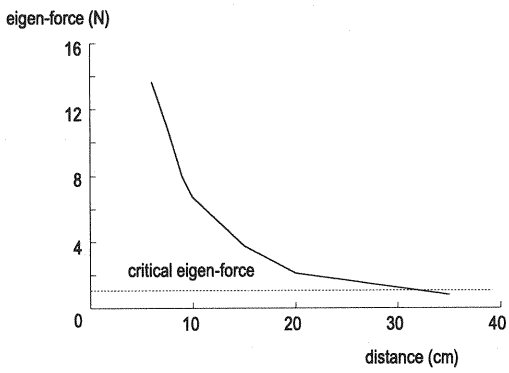

b) inverted eigen-force

Fig. 14 Data of Network Specification

5. CONCLUDING REMARKS

In order to develop a health monitoring system using the ACROSS technology, we carry out model experiments and numerical simulations, and obtain the following three are major findings: 1) it is shown in the model experiments that the initiation of defects can be detected if a suitable network of sources and receivers is used; 2) the FEM-based inversion, which is developed in the numerical simulations, can tell at least the location of a defects; and 3) details of the ACROSS monitoring system such as the arrangement of sources and receivers can be specified through numerical simulations. While future studies are definitely needed, these findings well support the potential applicability of the ACROSS health monitoring system to actual civil structures.

APPENDIX A SUMMARY OF ACROSS

The ACROSS technology attains a high S/N ratio by transmitting small but well-controlled harmonic signals and stacking data in a longer period. The

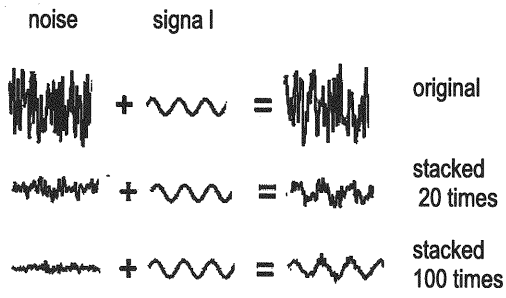

Fig. 15 Principles of ACROSS Technology

phase of signals and the stacking period must be accurately controlled. Even though received data include noises of larger magnitudes, noises with different frequencies or varying phases are excluded by repeating accurately controlled stacking. The configuration of harmonic signals (such as the amplitude, the phase or the wave form) cannot be changed by such stacking. **Figure** 15 shows a schematic view of stacking of random noises and signals of controlled harmonic waves.

G It should be mentioned that there are several projects in geophysics which make use of the ACROSS in order to investigate the geological structures. Nojima fault, a source of the Great Hanshin earthquake, is one target site, and a phased array system of ACROSS is being studied to obtain a clearer image of faults and their characteristics.

APPENDIX B MEASUREMENT ERROR

The following three are major factors that can produce large errors in the ACROSS measurement; 1) the frequency and location of input waves; 2) the accuracy in data stacking; and 3) the presence of initial imperfection. In the proposed inversion, measured data are used only to identify eigen-forces. Hence, even though the first two factors lead to incorrect eigen-forces, we can exclude such errors by setting a sufficiently large critical value for eigen-forces. That is, if a large eigen-force is computed at a certain part, we proceed to the second inversion which determines the degree of possible defects or damages. If not, that part is regarded as sound. To account for the third factor, we need to examine a change in the acceleration during a certain period. Such a change mainly represents the effects of newly formed defects, as the effects of imperfections or pre-existing defects can be eliminated by subtracting two data of the acceleration distribution. The above procedures may help the ACROSS that is used in monitoring fault activities since it is hard to verify the validity of the inversion for the fault problems.

REFERENCES

1) Committee of Solid Applied Mechanics: State and future of non-destructive evaluation in civil engineering, *JSCE*, 459/I-22, 1993.
2) Kumazawa, M. and Takei, Y.: Active method of monitoring underground structures by means of ACROSS, 1. Purpose and Principle, *Abstracts*, The Seismological Society of Japan, 2 (in Japanese), 1994.
3) Ha, D.H. and Higashihara, H.: Wave field generated by laterally vibrating source attached to the surface of elastic half-space, *JSCE*, 1997.
4) Tanaka, M. and Bui, H.D. (eds.): *Inverse Problems in Engineering Mechanics*, Springer, 1992.
5) Bui, H.D.: *Inverse Problem in the mechanics of materials: An introduction*, CRC Press, New York, 1994.
6) Kubo, S.: *Inverse Analysis*, Baifu-kan, 1992 (in Japanese).
7) Murakami, A.: Application of Inverse Analyses to Engineering Problems, *Theoretical and Applied Mech.*, Vol. 46, pp. 25-37, 1997.
8) Nishimura, N.: Crack Determination Problem, *Theoretical and Applied Mech.*, Vol. 46, pp. 39-57, 1997.
9) Hirose, S.: Inverse scattering for flaw type classification, in *Inverse Problems in Engineering Mechanics*, Springer, New York, pp. 359-366, 1992.
10) Tosaka, N. and Utani, A.: Identification analysis of elastic constants using Kalman filter-boundary element method, *J. of Struct. Eng.*, AIJ, No. 446, pp. 41-50, 1993 (in Japanese).
11) Okuno, T., Suzuki, M. and Honjo, Y.: Optimum groundwater modeling and identification of hydraulic conductivities based on ABIC and extended Kalman fiter algorithm, *Proc. JSCE*, 1997 (in print).
12) Sakurai, H., S. Akutagawa, and O. Tokutome: Inverse Analysis of Inelastic Strain Based on Norm Minimization, *JSCE*, 517/III-31, pp. 69-74, 1996.
13) Eshelby, J.D.: *Proc. Roy. Soc.*, Vol. A241, pp. 376-396, 1957.
14) Nemat-Nasser, S. and M. Hori: *Micromechanics: Overall Properties of Heterogeneous Materials*, North-Holland, London, 1993.
15) Hori, M. and Hosokawa, N.: Inverse Analysis Based on Equivalent Inclusion Method, *Proc. of Struct. Eng.*, 1997 (in press).
16) Hori, M., H. Goto and. S. Adatchi: Accurate Image Analysis on Failure Process of Ground Mold Reinforced by Gotextile, in *Symposium on Inverse Analysis and Construction Control in Geoengineering*, 151-156, 1997 (in Japanese).
17) Hori, M. and T. Kameda: Accurate Image Analysis on Failure Process of Ground Mold Reinforced by Gotextile, in *Symposium on Inverse Analysis and Construction Control in Geoengineering*, 151-156, 1997 (in Japanese).

(Received May 1, 1999)